

## Stable $(\text{Na}_{19})_2$ as a Giant Alkali-Metal-Atom Dimer

Susumu Saito and Shuhei Ohnishi

*Fundamental Research Laboratories, NEC Corporation, Miyazaki, Miyamae-ku, Kawasaki 213, Japan*  
(Received 22 April 1987)

We report that a dimer of clusters,  $(\text{Na}_{19})_2$ , is energetically stable and explains the abundance of  $\text{Na}_{38}$  in sodium-cluster mass spectra. A fusion process of two  $\text{Na}_{19}$  clusters has been studied on the basis of the jellium-sphere-background model by the local-spin-density-functional method. Calculated binding energies show that the force between two clusters is attractive and that the complete fusion is preceded by the formation of a stable  $(\text{Na}_{19})_2$ , whose electronic structure is analogous to an alkali-metal-atom dimer, supporting the concept of "clusters of giant atoms" for sodium clusters.

PACS numbers: 36.40.+d, 31.20.-d, 34.25.+t

Recent time-of-flight experiments for various metal clusters have revealed that electronic structures for metal clusters have shell structures.<sup>1-7</sup> A simple model,<sup>1</sup> in which the valence electrons of constituent atoms are assumed to be delocalized and bound in a spherical potential well, has been proposed to account for the shell structures. Observed mass spectra for monovalent metal clusters show peaks or steps at some cluster sizes, and the numbers of atoms in such abundant clusters are called "magic numbers." The numbers of electrons in these magic-number clusters are found to be equal to the shell-closing numbers of valence electrons.

In the case of sodium clusters,<sup>1,2</sup> there are some additional clear peaks which do not correspond to the shell-closing electronic structures. In our previous work,<sup>8</sup> it has been pointed out that some non-shell-closing magic numbers for sodium clusters can be interpreted in terms of clusters of giant atoms. The giant-atom concept for sodium clusters is also based on a shell model, in which clusters have such electronic energy levels as *s*, *p*, *d*, and so on, resembling ordinary atoms because of the spherical symmetry. For example, a  $\text{Na}_{19}$  cluster has a spherical core  $1s^2 1p^6 1d^{10}$  plus one  $2s$  electron. Hence,  $\text{Na}_{19}$  is expected to have properties similar to an alkali-metal atom. A dimer of alkali-metal atoms is known to be relatively stable because two valence electrons make a singlet pair in the bonding orbital. (Mass spectra for  $\text{Na}_n$ ,  $\text{K}_n$ , and  $\text{Na}_m\text{K}_{n-m}$  clusters<sup>2</sup> show peaks at  $n=2$ , which gives the shell-closing electronic structure  $1s^2$ . It is interesting that the shell model works even for such small clusters.) Therefore, two  $\text{Na}_{19}$  clusters should easily react during the adiabatic expansion of sodium gas in the time-of-flight experiment. This high reaction probability will make the non-shell-closing cluster  $\text{Na}_{38}$  abundant.<sup>2</sup> Some other examples of the giant atom have been proposed, and several clusters or molecules of giant atoms are found to explain the non-shell-closing magic numbers.<sup>8</sup>

In our recent work<sup>9</sup> based on a spherical-jellium-background model,<sup>10-13</sup> it has been found that two  $\text{Na}_4$  clusters attract each other strongly, and that

$\text{Na}_8$  clusters have properties similar to inert-gas atoms since two  $\text{Na}_8$  clusters are bound by a weak dispersion force. Hence,  $\text{Na}_8$  clusters scarcely react with other clusters, and many of them survive the adiabatic expansion. These results explain the strong peak of  $\text{Na}_8$  in the time-of-flight mass spectra and support the giant-atom concept. A spherical-jellium-background model also gives shell structures for valence electrons and makes it possible to discuss the relative stability of clusters in terms of their total energies. This success of the giant-atom concept indicates that reaction properties of sodium clusters can be explained by the analogy with reactions between ordinary atoms. Mass spectra for  $\text{Na}_n$  obtained in adiabatic expansion from sodium gas<sup>1,2</sup> have fine structures; that is, non-shell-closing abundant clusters and particularly poor clusters. In contrast, mass spectra for noble-metal clusters obtained by secondary-ion mass spectrometry (SIMS)<sup>3</sup> do not exhibit such fine structures. In the SIMS experiment, clusters come out directly from the surface-plasma region without cluster collisions. Hence, the fine structures of mass spectra for  $\text{Na}_n$  clusters in the adiabatic-expansion experiment reflect reaction processes of the clusters.<sup>14</sup>

In the present work, in order to see if sodium-cluster giant atoms make "giant molecules" or "giant clusters" statically, the reaction process in which two  $\text{Na}_{19}$  clusters evolve into one  $\text{Na}_{38}$  cluster has been studied with use of the jellium-sphere-dimer model. We have calculated the electronic structures and binding energies for the giant alkali-metal-atom dimer  $(X_{19})_2$ , and examined its stability. Here  $X_n$  is the model cluster for  $\text{Na}_n$  having the jellium-sphere background.

In the present calculation, electronic structures have been calculated in the local-spin-density-functional approximation (LDA)<sup>15-17</sup> with an exchange-correlation potential of the Ceperley-Alder type.<sup>18,19</sup> As for the basis functions, we have used the numerical eigenfunctions,  $1s$ ,  $1p$ ,  $1d$ ,  $2s$ , and  $1f$  for  $X_{19}$ , which have been located at both centers of two  $X_{19}$ . In addition, we have put the  $1s$ ,  $1p$ ,  $1d$ ,  $2s$ ,  $1f$ , and  $2p$  eigenfunctions for  $X_{38}$  at the center of the dimer  $(X_{19})_2$ . These jellium-sphere

eigenfunctions have also been obtained with use of LDA with the Ceperley-Alder potential.<sup>12</sup> To solve the Poisson equation and obtain the effective potential for electrons, the negative-charge density has been expanded by spherical harmonics  $Y_{lm}$  around the dimer center. The maximum value for  $l$  has been taken to be 8.

We have calculated the binding energies of  $(X_{19})_2$  relative to  $2X_{19}$ ,

$$E_b = E_{\text{tot}}((X_{19})_2) - 2E_{\text{tot}}(X_{19}), \quad (1)$$

for two different electronic configurations,  $(N_{\uparrow}, N_{\downarrow}) = (19, 19)$  and  $(20, 18)$ , and for  $25 \geq d \geq 2.0 \times 10^{-4}$  a.u. Here  $d$  is the interjellium distance; that is, the distance between two jellium centers, and  $N_{\sigma}$  is the number of the  $\sigma$ -spin electrons. Hereafter, the minimum  $d$  value  $2.0 \times 10^{-4}$  a.u. will be referred to as  $d=0$ , since it is very small, and  $d$  will be given in atomic units.

The radius of  $X_n$  is given by

$$R_n = n^{1/3} r_s, \quad (2)$$

where  $r_s$  is the Wigner-Seitz radius for bulk sodium, 3.93 a.u. In  $X_n$ , the positive charge is uniformly distributed  $[(\frac{4}{3}\pi r_s^3)^{-1}$  in atomic units] inside the sphere of radius  $R_n$ . Therefore, two jellium spheres of  $(X_{19})_2$  overlap for  $d < 2R_{19}$ . In this case, the two jellium spheres are enlarged equally so that the volume of the region inside the two spheres may be equal to  $\frac{8}{3}\pi(R_{19})^3$ , and the positive-background density inside the spheres

$$E_{\text{tot}} = E_{\text{kin}} + E_{\text{es}} + E_{\text{xc}}, \quad E_{\text{kin}} = \sum_{\nu, \sigma} \langle \Psi_{\nu\sigma} | -\frac{1}{2} \Delta | \Psi_{\nu\sigma} \rangle,$$

$$E_{\text{es}} = \frac{1}{2} \int d^3r \int d^3r' [\rho_-(\mathbf{r}) - \rho_+(\mathbf{r})][\rho_-(\mathbf{r}') - \rho_+(\mathbf{r}')]/|\mathbf{r} - \mathbf{r}'|, \quad (3)$$

$$E_{\text{xc}} = \int d^3r \epsilon_{\text{xc}}[\rho_{\uparrow}(\mathbf{r}), \rho_{\downarrow}(\mathbf{r})]\rho_-(\mathbf{r}).$$

Accordingly,  $E_b$  is given by the sum of three terms,

$$E_b = \Delta E_{\text{kin}} + \Delta E_{\text{es}} + \Delta E_{\text{xc}}. \quad (4)$$

In Eq. (3), the  $\nu\sigma$  sum is over the occupied spin orbitals,  $\Psi_{\nu\sigma}$ , which are obtained self-consistently in LDA, and  $\rho_+$ ,  $\rho_-$ , and  $\rho_{\sigma}$  are the positive-charge, negative-charge, and  $\sigma$ -spin densities, respectively.  $\epsilon_{\text{xc}}$  is the exchange-correlation energy per electron.

In Fig. 1, we show the binding-energy curves of  $(X_{19})_2$  for two electronic configurations,  $(N_{\uparrow}, N_{\downarrow}) = (20, 18)$  and  $(19, 19)$ . The ground-state configuration for  $d \geq 23$  is  $(20, 18)$ . At this relatively large distance, the interaction between two jellium spheres is rather weak and the electronic structure around each jellium sphere is close to that for the ground state of  $X_{19}$ , whose configuration is  $(N_{\uparrow}, N_{\downarrow}) = (10, 9)$ . When  $d \leq 22$ , the ground-state configuration for  $(X_{19})_2$  becomes  $(19, 19)$ . Around  $d = 16.5$ ,  $E_b$  for the ground state takes a minimum value,  $E_{m1}$ . From  $d = 12$  to 6, both  $(20, 18)$  and  $(19, 19)$  states

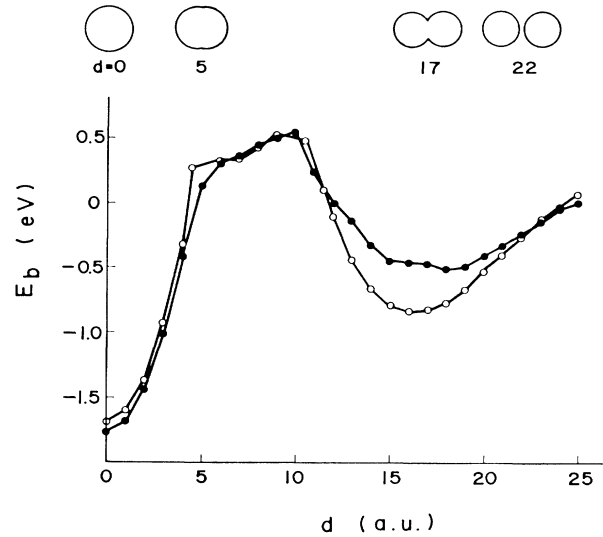


FIG. 1. Binding-energy curves of  $(X_{19})_2$  for two different electronic configurations,  $(N_{\uparrow}, N_{\downarrow}) = (20, 18)$  (filled circles) and  $(19, 19)$  (open circles). For several interjellium distances, schematic pictures for positive background are shown.

including the overlapping region is kept uniform,  $(\frac{4}{3}\pi r_s^3)^{-1}$ . By means of this procedure, a fusion of  $(X_{19})_2$  into  $X_{38}$  becomes a continuous process (Fig. 1).

Using the formulation given in our previous work,<sup>9</sup> we have calculated separately the kinetic energy  $E_{\text{kin}}$ , the electrostatic energy  $E_{\text{es}}$ , and the exchange-correlation energy  $E_{\text{xc}}$  for  $(X_{19})_2$  and  $X_{19}$ ,

take almost the same positive  $E_b$ . For  $d \leq 5$ , the ground-state configuration is again  $(20, 18)$  and its  $E_b$  takes a minimum value  $E_{m2}$  at  $d=0$ . Although the minimum at  $d=0$  is deeper than the minimum around  $d=16.5$ , they are separated by a high energy barrier, whose height relative to  $E_{m1}$  is about 1.4 eV. Moreover, the barrier has a positive energy value (about 0.5 eV). Hence, in a fusion process of two  $X_{19}$ , a stable dimer  $(X_{19})_2$  is formed around  $d = 16.5$ .

$\Delta E_{\text{kin}}$ ,  $\Delta E_{\text{es}}$ , and  $\Delta E_{\text{xc}}$  curves are shown in Fig. 2. In both configurations,  $\Delta E_{\text{kin}}$  and  $\Delta E_{\text{xc}}$  curves show a strong relationship with each other. When  $\Delta E_{\text{kin}}$  increases,  $\Delta E_{\text{xc}}$  decreases, and vice versa. For  $10 \geq d \geq 5$ ,  $\Delta E_{\text{kin}}$  and  $\Delta E_{\text{xc}}$  take the maximum and the minimum values, respectively. For the above interjellium distances, electrons occupy orbitals where they can well avoid each other because the potential from a positive background is far from a spherical one or the superposition of two

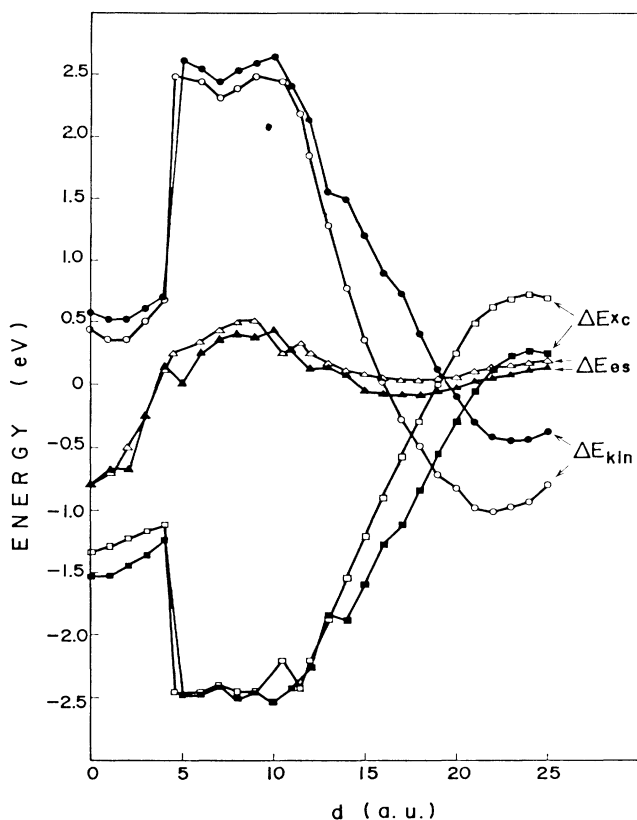


FIG. 2. Kinetic-energy (circles), electrostatic-energy (triangles), and exchange-correlation-energy contributions to binding energies. Filled circles, triangles, and squares are for  $(N_1, N_1) = (20, 18)$ , and open circles, triangles, and squares are for  $(19, 19)$ .

spherical potentials. Then, electrons gain correlation energy but lose kinetic energy.

It can be seen from Fig. 2 that the spin-nonpolarized state has lower  $E_b$  than the spin-polarized state around  $d=16.5$  because of the relatively large kinetic-energy gain. This implies that the spin-nonpolarized  $(X_{19})_2$  is bound by a covalent bond as in an alkali-metal-atom dimer.

Electronic energy levels of the spin-nonpolarized  $(X_{19})_2$  for several interjellium distances are shown in Fig. 3. At  $d=22$ , energy levels have little splittings and are nearly equal to the  $1s$ ,  $1p$ ,  $1d$ ,  $2s$ , and  $1f$  levels of  $X_{19}$  on account of a weak interaction between the two  $X_{19}$  spheres. At  $d=17$ , which is close to the equilibrium distance, the bonding and the antibonding levels originating from  $X_{19}$   $2s$  levels show a large splitting, and only the bonding level is occupied. Hence, we conclude that the stable  $(X_{19})_2$  is bound by a covalent bond of  $s$ -type orbitals in the same way as an alkali-metal-atom dimer. This result supports the presence of  $(Na_{19})_2$  as a giant alkali-metal-atom dimer, since  $E_b$  curves similar to

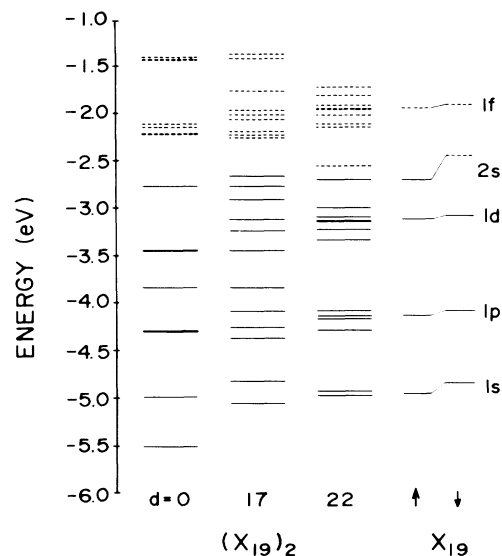


FIG. 3. Electronic energy levels for ground-state  $X_{19}$  and  $(X_{19})_2$  of  $(N_1, N_1) = (19, 19)$  with  $d=22, 17$ , and  $0$  a.u. Solid and dashed lines indicate occupied and unoccupied levels, respectively.

those in Fig. 1 are expected in a fusion of real  $Na_{19}$  clusters.

The present results confirm that two  $Na_{19}$  clusters react very easily because their electronic structure is similar to alkali-metal atoms, which explains the relatively high peak at  $Na_{38}$  in the mass spectra.<sup>1,2</sup> Since  $Na_{19}$  is an abundant cluster,  $Na_{38}$  also is abundant. Actually, in the adiabatic-expansion experiment,<sup>1</sup> larger clusters become abundant and smaller clusters are depleted when the carrier-gas pressure is increased. Hence, larger clusters are produced by coagulation of smaller clusters. The present results also show that the concept of "clusters of giant atoms" holds good in the case of a giant alkali-metal-atom dimer. Hence, we believe that other kinds of giant-atom clusters proposed previously<sup>8</sup> are also realistic. The giant-atom and the giant-atom-cluster concepts will be very useful in the consideration of the reaction of metal clusters.

We are greatly indebted to Dr. T. Inoshita for his valuable comments. We would like to thank Dr. Y. Ishii and Professor Marvin L. Cohen for their suggestions. We would like to express our gratitude to Dr. N. Watari for her help in developing computational programs.

<sup>1</sup>W. D. Knight, K. Clemenger, W. A. de Heer, W. A. Saunders, M. Y. Chou, and M. L. Cohen, Phys. Rev. Lett. **52**, 2141 (1984).

<sup>2</sup>W. D. Knight, W. A. de Heer, K. Clemenger, and W. A. Saunders, Solid State Commun. **53**, 445 (1985).

<sup>3</sup>I. Katakuse, T. Ichihara, Y. Fujita, T. Matsuo, T. Sakurai,

and H. Matsuda, *Int. J. Mass Spectrom. Ion Processes* **67**, 229 (1985).

<sup>4</sup>W. D. Knight, K. Clemenger, W. A. de Heer, and W. A. Saunders, *Phys. Rev. B* **31**, 2539 (1985).

<sup>5</sup>K. Clemenger, *Phys. Rev. B* **32**, 1359 (1985).

<sup>6</sup>W. A. Saunders, K. Clemenger, W. A. de Heer, and W. D. Knight, *Phys. Rev. B* **32**, 1366 (1985).

<sup>7</sup>M. M. Kappes, M. Schar, P. Radi, and E. Schumacher, *J. Chem. Phys.* **84**, 1863 (1985).

<sup>8</sup>S. Saito and S. Ohnishi, in *Proceedings of the International Symposium on the Physics and Chemistry of Small Clusters, Richmond, Virginia, 1986*, edited by P. Jena, B. K. Rao, and S. N. Khanna (Plenum, New York, 1987).

<sup>9</sup>Y. Ishii, S. Saito, and S. Ohnishi, to be published.

<sup>10</sup>W. Ekardt, *Phys. Rev. B* **29**, 1558 (1984).

<sup>11</sup>M. Y. Chou, A. Cleland, and M. L. Cohen, *Solid State*

*Commun.* **52**, 645 (1984).

<sup>12</sup>Y. Ishii, S. Ohnishi, and S. Sugano, *Phys. Rev. B* **33**, 5271 (1986).

<sup>13</sup>B. K. Rao, P. Jena, M. Manninen, and R. M. Nieminen, *Phys. Rev. Lett.* **58**, 1188 (1987).

<sup>14</sup>Attempts to explain the relative abundances of clusters from the viewpoint of the cluster-growth kinetics have been made for carbon clusters [J. Bernholc and J. C. Phillips, *Phys. Rev. B* **33**, 7395 (1986)] and for argon clusters [S.-N. Yang and T.-M. Lu, *Phys. Rev. B* **35**, 6944 (1987)].

<sup>15</sup>P. Hohenberg and W. Kohn, *Phys. Rev.* **136**, B864 (1964).

<sup>16</sup>W. Kohn and L. J. Sham, *Phys. Rev.* **140**, A1133 (1965).

<sup>17</sup>U. von Barth and L. Hedin, *J. Phys. C* **5**, 1629 (1972).

<sup>18</sup>D. M. Ceperley and B. J. Alder, *Phys. Rev. Lett.* **45**, 566 (1980).

<sup>19</sup>J. P. Perdew and A. Zunger, *Phys. Rev. B* **23**, 5048 (1981).